ACADEMIC PRESS

Available online at www.sciencedirect.com
SCIENCE DIRECT®

Journal of Catalysis 214 (2003) 200–212

JOURNAL OF CATALYSIS

www.elsevier.com/locate/jcat

Construction of a reaction coordinate and a microkinetic model for ethylene epoxidation on silver from DFT calculations and surface science experiments

Suljo Linic and Mark A. Barteau *

Center for Catalytic Science and Technology, Department of Chemical Engineering, University of Delaware, Newark, DE 19716, USA

Received 22 July 2002; revised 6 November 2002; accepted 11 November 2002

Abstract

Density functional theory (DFT) calculations have been used to investigate a possible reaction coordinate for the epoxidation of ethylene on silver. These studies have been motivated by recent advances in the understanding of the mechanisms of olefin epoxidation. We find various surface intermediates and transition states along the reaction coordinate with structures, binding energies, and vibrational frequencies that are in good agreement with experimental results. We also discuss the uniqueness of silver in providing an optimal environment for highly selective ethylene epoxidation. It was concluded that ethylene reacts with adsorbed oxygen to form a surface intermediate, identified as a surface oxametallacycle. This intermediate reacts through a transition state to form gas-phase ethylene oxide. The kinetic and thermodynamic parameters obtained in these studies are used to formulate a simple microkinetic model. The microkinetic model is used to estimate parameters needed for the formulation of a rate law. The resulting rate law agrees very well with observations from macroscopic measurements of ethylene epoxidation rates under steady-state conditions.

Keywords: Ethylene epoxidation; Ethylene oxide; Oxametallacycle; Density functional theory

1. Introduction

The epoxidation of ethylene to form ethylene oxide is one the most important heterogeneous catalytic oxidation processes. The process employs a silver catalyst supported on α-Al_2O_3 and promoted by alkalis and halides. Considerable effort has been devoted to understanding the mechanism of silver-catalyzed ethylene epoxidation [1]. Nearly all available surface science techniques have been used to investigate the elementary steps of this reaction. A molecular-level understanding of this reaction is still lacking since the different reacting species are not easily probed during the reaction. It has been suggested that the surface-mediated addition of ethylene to oxygen is the rate-determining step [2]. This addition is followed by a number of rapid steps, making it difficult to track intermediates formed in these steps by spectroscopic techniques. One way to circumvent this problem is to induce an elementary surface reaction by an STM tip. This can be done by manipulating adsorbates using voltage pulses at low temperatures where intermediates are stable enough—i.e., are "frozen in time" [3]—to be probed by different surface science techniques. This approach has been implemented by Hahn and Ho [4] in their analysis of the oxidation of CO to form CO_2 on Ag(110).

Another way to reach a microscopic understanding of the sequence of elementary steps by which a product is formed is to isolate and identify the intermediates that are thermodynamically and kinetically accessible using traditional surface science techniques, such as temperature programmed desorption (TPD) and high-resolution electron energy loss spectroscopy (HREELS). Quantum mechanical computational tools, such as density functional theory (DFT), may then be used to construct a reaction coordinate that is in accord with experimental observations. This approach allows determination of not only the surface intermediates but also the relevant transition states along the reaction coordinate. The understanding of surface–adsorbate interactions in this way, with the adsorbates being either surface intermediates or transition states, is crucial in the design of new or improved catalysts from first principles.

* Corresponding author.
E-mail address: barteau@che.udel.edu (M.A. Barteau).

0021-9517/03/$ – see front matter
doi:10.1016/S0021-9517(02)00156-2

In this work we report experimentally motivated DFT calculations of the reaction coordinate for silver-catalyzed epoxidation of ethylene to form ethylene oxide. In the first section of this report we highlight a few important experimental observations. This is followed by the description of the calculation method and the results obtained in the calculations. As will be shown, important parallels can be drawn between the experimental and computational results. These results provide additional insights into the unique ability of silver to selectively oxidize ethylene to form ethylene oxide and suggest key principles that govern rational design of epoxidation catalysts.

2. Summary of previous experimental results

A large number of very detailed experiments have been aimed at understanding the elementary steps that take place in ethylene epoxidation. In this report we do not attempt to review all of these, but rather we emphasize a few results that we believe provide a reasonable cross-section of experimental observations.

As stated above, the first step in our approach was to isolate and identify thermodynamically and kinetically accessible surface intermediates. The identification of relevant intermediates often relies on different electron spectroscopies performed under UHV conditions. However, in UHV surface science experiments it is often difficult to isolate surface intermediates that are relevant for catalytic processes. This is particularly the case for processes in which the rate-limiting step, defined as the step that involves overcoming the highest energy barrier along the reaction coordinate, occurs at the front end of the reaction coordinate. A schematic reaction coordinate for such a process is shown in Fig. 1. After *A* and *B* are adsorbed onto a surface they react in the rate-determining step to form *C*(ads). In order to form *C*(ads), the system has to be supplied with the energy to overcome the barrier for *C*(ads) formation. This energy precludes a "long life" of any other intermediate, such as *C*(ads) or *D*(ads) in Fig. 1, formed subsequent to the crossing of this barrier. In such cases it may be possible to take advantage of the principle of microscopic reversibility to generate surface intermediates from the reaction product on the surface, i.e., via the reverse reaction. In the case of the schematic reaction coordinate shown in Fig. 1, this approach would allow the isolation and spectroscopic identification of *D*(ads), assuming that there are no other accessible reaction pathways by which this intermediate can easily dissociate. We take advantage of this strategy in the analysis of the reaction of ethylene and oxygen to form ethylene oxide on Ag. In our recent contribution [5] ethylene oxide was adsorbed onto the Ag(111) crystal plane at $\sim$ 250 K. This resulted in ethylene oxide ring-opening and the formation of a stable surface intermediate which reacted at $\sim$ 310 K to reform ethylene oxide plus water and ethylene. By comparing HREELS experiments and DFT calculations it was shown that this surface intermediate is the surface oxametallacycle shown in Fig. 2. This result presents the first link between a spectroscopically identified stable surface intermediate and ethylene oxide and provides a feasible pathway for epoxide formation. It is also important to note that a surface intermediate with an almost identical vibrational fingerprint appeared in steady state ethylene epoxidation with a supported silver catalyst [6], thus providing an important link between surface science and catalytic experiments.

Another issue in the formulation of the reaction coordinate is the role of oxygen in the ethylene epoxidation process. Although one still finds occasional assertions that adsorbed dioxygen is the active oxidation species [7], it is generally accepted that atomic adsorbed oxygen is the active species in the epoxidation of ethylene [1,2]. In experiments in which atomic oxygen was co-adsorbed with ethylene, Grant and Lambert concluded that molecular oxygen has no direct role in either partial or complete oxidation. These arguments are further supported by the observation that yields of ethylene oxide can exceed the stoichiometric limit (6/7 stoichiometry) if molecular oxygen is assumed

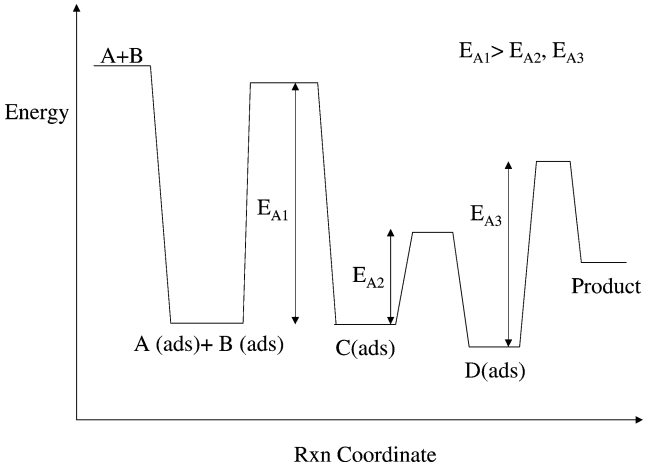

Fig. 1. Hypothetical reaction coordinate in which isolation of *C*(ads) and *D*(ads) in UHV by the direct route is precluded.

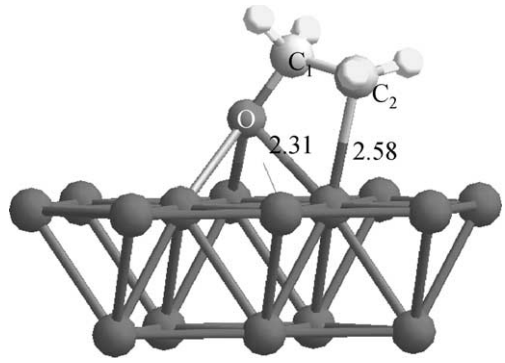

Fig. 2. Structure of the surface intermediate isolated and spectroscopically identified on Ag(111) upon activated adsorption of ethylene oxide [5]. This intermediate reacted at 310 K to reform ethylene oxide plus minor products, water, and ethylene.

Table 1
Stereospecificity of oxidation of *cis*- and *trans*-1,2-d_2-ethylene

System	Ethylene isotopomer oxidized	Epoxide composition	
		cis (%)	*trans* (%)
Cant[a]	*cis*-$C_2H_2D_2$	53.4	46.6
Flow System	*trans*-$C_2H_2D_2$	45.8	54.2
Cant[b]	*cis*-$C_2H_2D_2$	53.8	46.2
Recirculating	*trans*-$C_2H_2D_2$	45.9	54.1
Richey[c]	*cis*-$C_2H_2D_2$	70 ± 5	30 ± 5
Recirculating	*trans*-$C_2H_2D_2$	32 ± 5	68 ± 5

[a] At 187 °C [10].
[b] At 168 °C [10].
[c] Temperature is not known [12].

Table 2
Binding energies for O atom adsorbed on Ag(111) with respect to gas phase O_2 in kcal/mol

Calculation method	DZ on Ag_{15}	DZP on Ag_{15}	TZPP on Ag_{15}	Pseudo-potential plane wave $p(2 \times 2)$
Binding energy (kcal/mol, O)	−18	−2.5	0.2	−7.5[a]

The more negative number indicates a higher stability. The energies are obtained using $\Delta H_{\text{rxn}} \cong \Delta E_{\text{rxn}} = E(\text{surface complex}) - E(\text{cluster}) - \frac{1}{2}E(O_2)$ for cluster, and $\Delta H_{\text{rxn}} \cong \Delta E_{\text{rxn}} = E(\text{surface complex}) - E(\text{metal unit cell}) - \frac{1}{2}E(O_2)$ for pseudo potential plane wave calculations. From TPD experiments Campbell et al. [58] estimated the bond energy for O(ads) with respect to oxygen molecule to be ~ -11 kcal/mol.
[a] Ref. [25].

to be the active species [8]. It was also observed by Grant and Lambert that reaction of deuterated ethylene with adsorbed oxygen on Ag(111) led to an increase in the selectivity to epoxidation products relative to complete oxidation products; this and similar results on supported catalysts have been explained in terms of a common surface intermediate responsible for both processes [9,10].

Another interesting result is that there is relatively little retention of configuration reported in previous studies of epoxidation of either *cis* or *trans* 1,2-d_2-ethylene [10–12]. The results of these experiments are summarized in Table 1. This observation indicates that, at some point along the reaction coordinate, rotation about the C–C bond in ethylene has to be possible. This argues against concerted addition of surface oxygen to the C=C bond of ethylene. It is important to note that Cant and Hall also concluded in their studies that the loss of initial configuration was due neither to isomerization of deuterated ethylene prior to oxidation nor to isomerization of the epoxide subsequent to its formation [10].

3. Computational methods

The Amsterdam density functional (ADF) program [13,14] was used for all reported cluster calculations. The Kohn–Sham one-electron equations are solved by expanding the wave functions in Slater-type atomic orbitals using the Vosko–Wilk–Nusair (VWN) functional [15]. All calculations were spin-unrestricted and employed Becke [16] and Perdew [17] gradient approximations for the exchange and correlation energy terms, respectively. The calculations were performed on Ag_{15} clusters using a DZ (double zeta basis set), DZP (double zeta basis set with polarization functions used for H, C, and O but not for Ag), and TZPP (triple zeta basis set with doubly polarized basis functions for H, C, and O but not for Ag) on Ag_{15}. The results of different basis set calculations are within ± 3 kcal/mol for energies of different surface intermediates with respect to each other. We also observed that there exists a significant discrepancy in the results of calculations with different basis sets when comparing gas phase molecules (O_2 and EO) with the adsorbed states of these molecules (O(ads) and the oxametallacycle, respectively), as shown in Table 2. These discrepancies are resolved by comparing the predicted binding energies to the experimentally measured ones.

The optimized geometries and respective energies of surface intermediates were calculated as described previously [18]. In calculating the transition states the following procedure, consistent with transition state theory, was implemented:

(i) A geometry of the transition state is proposed based on the geometries of the reactant and product in a particular elementary step.
(ii) The transition state in question is then optimized. This optimization is done by moving along the potential energy surface and calculating the energy gradients and Hessian for each geometry on this path. The transition state is optimized when a point is reached where the energy gradient vanishes and the Hessian has one imaginary value.
(iii) Frequency calculations are performed on the optimized transition state, thus verifying that there is only one imaginary frequency corresponding to the normal mode that identifies the reaction coordinate.
(iv) The optimized transition state is slightly perturbed along the reaction coordinate, corresponding to the normal mode with imaginary frequency, in the direction of the product or reactant.
(v) The perturbed transition state geometries obtained in step (iv) are then optimized, yielding respective geometries of the product or reactant in the particular elementary step.

A similar approach has been prescribed by van Santen [19] and previously implemented successfully for reactions of various oxametallacycles on silver surfaces [20]. To obtain vibrational spectra of the surface intermediates and transition states, two-point frequency calculations using an integration accuracy of 10^{-6} were performed on these structures.

We have also used periodic DFT calculations to confirm the accuracy of cluster calculations. Periodic plane wave

calculations are expected to be superior to cluster calculations in their ability to capture electronic properties of extended surfaces. Periodic DFT calculations were therefore used to calculate optimized geometry and binding energies of the relevant stable surface intermediates. The code used in these studies was DACAPO [21]. The GGA-PW91 exchange correlation was employed. The electronic density was determined by iterative diagonalization of the Kohn–Sham Hamiltonian. The ionic cores were represented by ultrasoft pseudopotentials, a plane wave basis set (Ecut = 25Ry). The silver surface was simulated by using a two-layer bulk-terminated slab of static silver. The relaxations of the surface atoms led to increases in adsorbate stabilities by ~ 2 kcal/mol. We have also performed a few geometry optimizations on four-layer bulk-terminated slabs without observing significant differences in the stability of surface intermediates with respect to each other. The slabs are separated by six atomic layers (approximately 15 Å) of vacuum. The difference in the work function between the two slab surfaces is corrected by adding a dipole layer of appropriate magnitude in the middle of six vacuum layers. The lattice constant for silver employed in these calculations was equal to the experimentally determined value of 4.09 Å. The same lattice constant was used in the cluster calculations. Surface Brillouin zone integration was done on a special 18k-points grid. In all simulations a molecule was adsorbed on a $p(2 \times 2)$ unit cell, corresponding to a coverage of 0.25 monolayers.

Periodic DFT calculations can also be used to calculate the geometries and binding energies of the relevant transition states. In this work we use the transition states obtained from the cluster calculations as a starting geometry for the slab calculations. Since the forces on the atoms in the starting transition state geometries are calculated to be mostly in the z-direction, these structures are allowed to move up or down until the forces acting on different atoms are minimized. The transition states were considered to be optimized when the convergence threshold of 0.2 eV/Å was reached for the forces in all directions.

We report energies and geometries calculated using TZPP basis sets for cluster calculations and periodic DFT calculations, unless specified otherwise. The energies of all surface structures are calculated with respect to the energy of adsorbed oxygen and gas phase ethylene as

$$\Delta H_{\mathrm{rxn}} \cong \Delta E_{\mathrm{rxn}} = E(\text{surface structure}) - E(\text{ethylene}) - E(\text{adsorbed oxygen}), \quad (1)$$

where E(surface structure) is the energy of the surface species bonded to metal cluster or metal unit cell. E(adsorbed oxygen) represents the energy of the system in which an oxygen atom is adsorbed onto the cluster or the metal unit cell, while E(ethylene) is the energy of ethylene molecule in the gas phase.

4. Results

Since it is well established that atomic, rather than molecular, oxygen is the active species in ethylene epoxidation, we assume that the first step along the reaction coordinate will include the adsorption and dissociation of molecular oxygen. The question of adsorption and dissociation of oxygen on Ag has previously been investigated experimentally [22] and theoretically [23–26]. Recent calculations suggest that the dissociation of oxygen on silver is activated, with activation energies of ~ 37 kcal/mol on Ag(111) and ~ 17 kcal/mol or 6 kcal/mol on step sites, depending on the functional used [25]. The higher barrier on step sites was obtained using the RPBE (revised Perdew–Burke–Ernzehof functional), while the lower barrier was obtained using PW91. These differences most likely arise from discrepancies in the calculation of the energy for the gas phase molecule. Different activation barriers for oxygen dissociation and their impact on our analysis will be discussed latter in the report. The relative magnitudes of the barriers noted above would suggest that under reaction conditions the dissociation of oxygen takes place mostly on stepped sites. The enthalpy of reaction for oxygen dissociation on Ag(111) is estimated to be about -8 kcal/mol for a Ag(111)-terrace and about -15 kcal/mol for a Ag-step [25]. The addition of the activation energy for oxygen dissociation and the enthalpy of reaction yields 45 and 32 kcal/mol per oxygen molecule for the activation barriers for oxygen atom recombination and desorption from Ag(111)-terrace and Ag-step sites, respectively. These values are in excellent agreement with the values reported for different silver planes and silver powders, which range from 30 to 44 kcal/mol [27–31].

The transition state for dissociative adsorption of O_2 on Ag is calculated to be product-like; i.e., the O–O bond length in the transition state is quite long and the bond order is greatly reduced [25]. In another theoretical study, Li et al. [26] have shown that the binding energy of oxygen on silver depends strongly on the surface coverage, even at low coverages. This is not surprising since it is known that oxygen induces a significant change in the silver work function caused by a dipole that can induce long-range repulsive electrostatic adsorbate–adsorbate interactions. For example, Li et al. calculated that the binding energy at 0.11 monolayer is greater (more stable) by 5 kcal/mol per O_2 molecule than at 0.25-monolayer oxygen coverage [26]. This information, coupled with the product-like nature of the transition state, implies that the activation energy for oxygen dissociation is coverage-dependent and that lower activation barriers are to be expected at lower coverages.

In the energetically optimized structure, an oxygen atom resides in a threefold hollow site with its center approximately 1.3 Å above the plane defined by the centers of the surface silver atoms. The O atom on a Ag cluster is modeled as adsorbed in a FCC site. This site is found to be isoenergetic to the HCP site and these are the preferred sites for

the adsorption of O on the Ag surface, as determined by our DFT calculations.

The next step along the reaction coordinate is the adsorption of ethylene onto the oxygen-covered Ag surface. Ethylene is found to desorb at ∼ 140 K on Ag surfaces in UHV, indicative of a weak interaction (ca. 8–9 kcal/mol) between ethylene and the Ag surface [32–34]. This weak interaction suggests that, under reaction conditions ($T > 200\,^{\circ}$C), ethylene molecules are in a state of motion, being continuously adsorbed and desorbed from a weakly bound state on a surface. On the other hand, the activation energy for desorption of oxygen molecules from the surface is much higher, about 32–45 kcal/mol, depending on surface plane. This difference in the respective oxygen and ethylene stabilities on Ag suggests that under reaction conditions weakly adsorbed, mobile ethylene approaches an oxygen-covered Ag site. It has also been shown in extensive calculations of oxygen adsorption on Ag(001) [35] that the diffusion of oxygen from the most stable hollow site to another hollow site requires only ∼ 20 kcal/mol (i.e., about one-half the recombination desorption barrier), suggesting that under reaction conditions the diffusion of oxygen atoms on the surface is likely to take place.

As ethylene approaches the oxygen-covered sites on the Ag surface, the interaction between ethylene carbon atoms and oxygen adatoms takes place. This interaction results in the formation of a transition state (TS1), shown in Fig. 3. The arrows represent the dominant motion of reacting species corresponding to the movement along the reaction coordinate, i.e., to the mode exhibiting an imaginary frequency in the DFT calculations for the transition state. The reaction coordinate is dominated by the approach of the C_1 carbon to oxygen. It is also observed that the C–C bond is elongated from 1.33 Å for gas phase ethylene to 1.38 Å for the transition state, consistent with the expected decrease of the C–C bond order. Also, the C_1–O bond is being formed in the transition state, as evidenced by the change in the hybridization of the C_1 carbon from sp^2 to sp^3 with perturbation of the planar configuration corresponding to gas-phase ethylene. The activation energy for the addition of ethylene from a weakly bound state to oxygen on the surface is calculated by subtracting the energy of the adsorbed oxygen plus weakly bound ethylene system from the energy of TS1. The activation energy for this elementary step is found to be 14.9 kcal/mol as calculated by cluster and periodic DFT calculations and accounting for 8 kcal/mol for the heat of ethylene adsorption.

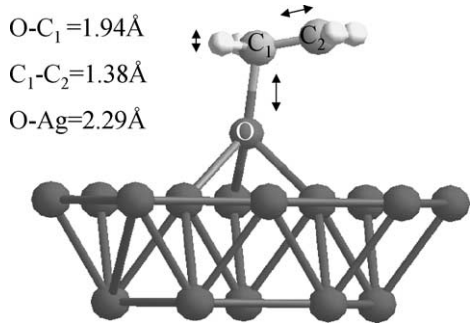

Fig. 3. Structure of transition state 1 (TS1) for elementary step 1. Ethylene reacts with an oxygen-covered surface site. The arrows represent the normal mode associated with the reaction coordinate for this elementary step.

The next step is to determine the product of this elementary step. This is done by slightly perturbing the structure of the calculated transition state along the direction of the reaction coordinate. This direction is inferred from the normal mode that corresponds to the imaginary frequency of TS1. The perturbation is done by simulating the normal mode of TS1 with imaginary frequency and then freezing its geometry when the maximum change in a bond length or a bond angle that dominates the imaginary normal mode is ∼ 5% with respect to the transition state geometry. For example, the O–C_1 stretch dominates the normal mode associated with this elementary step of TS1. We perturb the transition state structure by changing the O–C_1 bond length from 1.94 to 1.86 Å and adjusting all other atom positions accordingly. The perturbed transition state geometry is then optimized, with no geometric constraints imposed on the structure (i.e., every atom, other than the Ag atoms, is free to move in all directions); the optimization leads to a stable surface intermediate. This intermediate is the product of the elementary step that proceeds via TS1.

The structure of this surface intermediate, as calculated by periodic DFT, is shown in Fig. 4. This surface intermediate is similar to the surface intermediate that we spectroscopically identified during dissociative adsorption of ethylene oxide on Ag(111) [5], with the calculated structure shown in Fig. 2. The major difference is that the O–C_1–C_2 angle is 116° in the structure in Fig. 4 compared to 112° for the structure in Fig. 2. This results in the oxygen of the oxametallacycle residing more nearly in a bridging site (Fig. 4) vs a three-fold hollow site (Fig. 2). Both structures have been

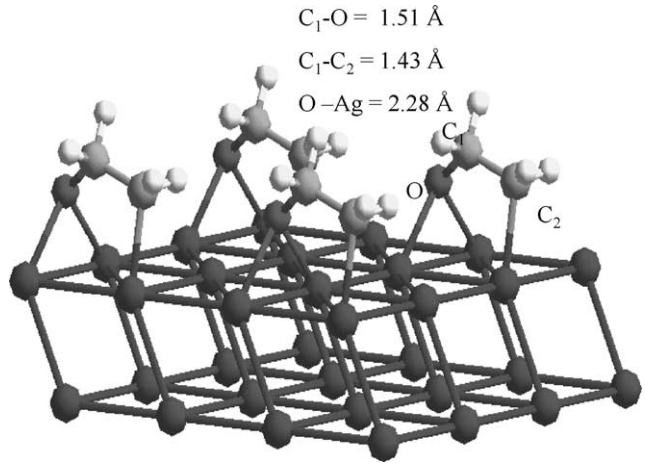

Fig. 4. The product of the elementary step 1. Adsorbed oxygen and ethylene react to form a cyclic surface structure. The geometry of the surface intermediate is calculated using the pseudo-potential plane wave method that takes advantage of the surface translational symmetry.

generated experimentally in our previous studies. The structure shown in Fig. 2 was identified in the reversible ring opening of ethylene oxide on Ag(111) [5]. The structure shown in Fig. 4 was isolated and spectroscopically identified in the reaction of 2-iodoethanol on Ag(111) [36] and Ag(110) [37]. This intermediate reacted to form mostly acetaldehyde. However, our calculations for both clusters and slabs suggest that there is little activation barrier to the interconversion of the structures illustrated in Figs. 2 and 4, and therefore both might be expected to lead to ethylene oxide. The absence of ethylene oxide from the product slate of oxametallacycles synthesized from iodoethanol may reflect the influence of the co-adsorbed iodine atoms on the reactions of these intermediates, rather than intrinsic reactivity differences between apparently similar intermediate structures.

In Fig. 4 it is observed that the C_1–O bond has been formed. This is evidenced by the sp^3 hybridization of C_1 and also by the movement of oxygen farther away from the Ag surface. This movement of O is a consequence of the weakening of the Ag–O bonds, which can be explained using bond order conservation arguments [38]. The concept of bond order conservation has been found to be extremely useful when dealing with adsorption and reaction on surfaces. It is worth noting that even though bond order conservation is an empirical method, similar arguments can be derived from more theoretical viewpoints, such as "effective medium theory" [39] and the idea of "total overlap population" [40].

Earlier work by Somorjai and co-workers [41] and Hoffmann and co-workers [42] suggested a model for the binding of hydrocarbons to close-packed transition metal surfaces. It was suggested that carbon binds to the surface in a position that would allow it to complete its tetravalency. If we assume that the C_2 carbon atom in the –O–C_1–C_2– backbone, shown in Fig. 4, behaves similarly to a carbon in a simple hydrocarbon fragment, we would expect the terminal carbon of the –O–C–C– backbone to bond atop a surface metal atom and complete its tetravalency, consistent with the structure shown in Fig. 4. The same calculations shown for periodic slabs in Fig. 4 were performed using Ag clusters as well. The geometry of the structure converged in our cluster calculations using the TZPP basis set is almost identical to the geometry converged in the pseudo-potential plane wave calculations. This suggests that interactions between oxametallacycles at a coverage of one-quarter monolayer do not significantly perturb their structures.

The next step in the development of the reaction coordinate is to locate a transition state that leads to the formation of ethylene oxide from the surface intermediate in Fig. 4. Extensive DFT calculations showed that the formation of ethylene oxide from the surface intermediate in Fig. 4 involves two characteristic motions. The first is the motion of the weakly bound carbon, C_2, away from the Ag surface. The approach of C_2 and the oxygen atom leads through transition state TS2, shown in Fig. 5, to the formation of ethylene oxide. The arrows in Fig. 5 depict motion along the reaction coordinate by which ethylene oxide is formed. Again, this

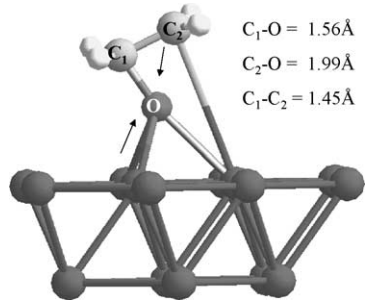

Fig. 5. Transition state 2 (TS2). This transition state is involved in the formation of ethylene oxide from the structure shown in Fig. 4. The arrows represent the reaction coordinate for this elementary step.

reaction coordinate represents the motion corresponding to the imaginary frequency calculated in the vibrational spectrum of TS2. Careful examination of TS2 clearly suggests the formation of a ring structure. The C_2–O bond is beginning to form and also the O–Ag bonds are elongating, suggesting that the product of this elementary step is gas-phase ethylene oxide, which was confirmed by the calculations.

In Fig. 6 we show a complete reaction coordinate incorporating the energies associated with each elementary step. The reported energies reflect the overall reaction with the following molarities: dissociative adsorption of molecular oxygen to form two oxygen atoms,

$$O_2 + 2^* \rightarrow 2O^*,$$

and the surface reactions of adsorbed oxygen and weakly adsorbed ethylene to form ethylene oxide via a surface oxametallacycle intermediate,

$$C_2H_4{}^* + O^* \rightarrow C_2H_4O.$$

It is important to note that the local minima (stable intermediates) and local maxima (transition states) on the potential energy surface have been calculated using a rigorous mathematical procedure that emerges from transition state

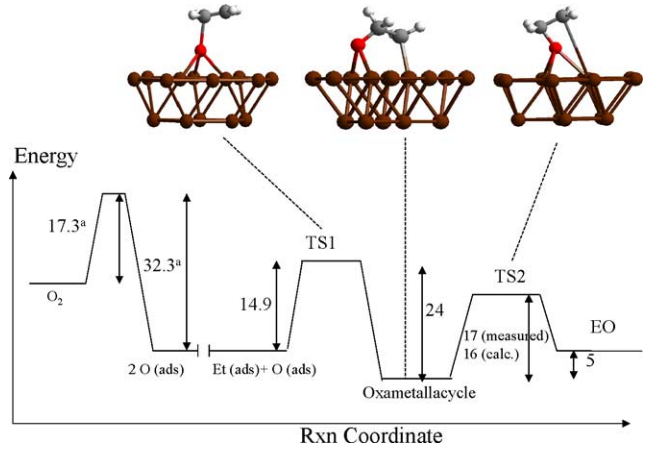

Fig. 6. Calculated reaction coordinate for ethylene epoxidation on silver. Energy units are kcal/mol. The discontinuity in the reaction coordinate reflects the change in oxygen molarity. The barrier for oxygen dissociation is from [25].

theory, and that their geometries are expected to be fairly accurate. In the next section we analyze the reaction coordinate, shown in Fig. 6, with respect to experimental observations.

5. Discussion

The focal point of this section is the consideration of how the reaction coordinate, constructed in Fig. 6, can explain experimental observations, and whether it provides any clues that would help understand the unique ability of silver to catalyze ethylene epoxidation. We also discuss the requirements for an efficient epoxidation catalyst.

5.1. Reaction coordinate

The reaction coordinate in Fig. 6 explains why it is possible to ring open ethylene oxide and then reform it from the isolated stable surface intermediate shown in Fig. 2, as observed experimentally on the Ag(111) surface [5]. If the reaction coordinate is traced from the product ethylene oxide, it is observed that the activation energy for ring-opening ethylene oxide is about 11 kcal/mol. After ring opening, formation of a surface intermediate that is stable with respect to the gas-phase ethylene oxide is predicted, which we observed experimentally [5]. This intermediate is now confined within an energy well and 17 kcal/mol is needed to overcome the barrier and reform ethylene oxide, while at least 24 kcal/mol is required to break the C_1–O bond and form adsorbed ethylene plus adsorbed oxygen. This energy difference results in the preferred formation of ethylene oxide as the temperature of the surface intermediate in our TPD experiments increases. The reason that in experiments that involve adsorption and reaction of ethylene oxide on Ag(111) we isolate the surface oxametallacycle intermediate is simply that it is thermodynamically and kinetically the most stable accessible intermediate along the reaction coordinate. The proposed reaction coordinate also explains the relatively narrow window of temperature in which this species can be isolated by ring opening ethylene oxide. At adsorption temperatures significantly lower than 250 K, ethylene oxide does not ring open since the activation energy required for this process is $\sim$ 11 kcal/mol. At adsorption temperatures significantly higher than 250 K no intermediate along the reaction coordinate is stable enough to survive on the silver surface for an extended period of time; i.e., multiple reaction pathways would be activated, resulting in the desorption of the products formed in these reactions. It is also important to note that the activation energy experimentally determined [5] for the ring closure of the structure shown in Fig. 4 is $\sim$ 17 kcal/mol, in excellent agreement with the activation energy calculated for this elementary step (16 kcal/mol).

Further analysis of the reaction coordinate in Fig. 6 also offers a possible explanation concerning the lack of retention

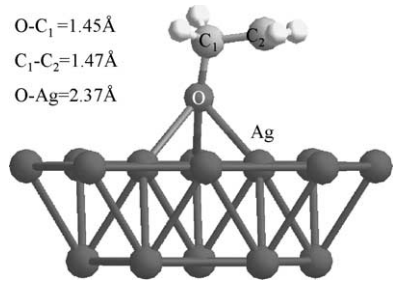

Fig. 7. Surface intermediate possibly responsible for an energetically feasible rotation about the C–C bond. This rotation may produce the experimentally observed mixture of *cis* and *trans* epoxides even when the reactant contains only one olefin isomer.

of configuration upon epoxidation of either *cis* or *trans* 1,2-d_2-ethylene [10–12]. As stated above, the elementary step that results in EO formation from the surface intermediate shown in Fig. 4 can be explained as scission of the C_2–Ag bond accompanied by the formation of C_2–O bond. Along this path there are multiple adsorbate geometries that might allow for energetically inexpensive rotation about the C_1–C_2 bond. We have selected one of these geometries shown in Fig. 7 and calculated the energy required for rotation to take place. We have not performed rigorous TS search calculations for the rotation step, but to a first approximation we can assume that the upper limit for the rotation activation energy can be calculated just by rotating the C_1–C_2 bond by 90° and determining the single point energy for that geometry. This calculation shows that the upper limit for the activation energy of rotation is $\sim$ 2 kcal/mol. This suggests that under reaction conditions rotation about the C_1–C_2 bond might be possible. This rotation would result in a distribution between *cis* and *trans* configurations, as is experimentally observed. The structure shown in Fig. 7 is generated on the surface as the C_2–Ag bond is broken in the process of converting the structure shown in Fig. 4 into EO along the reaction coordinate en route to TS2. This structure can be visualized on the potential energy surface as a "shelf" with a small change in energy along the reaction coordinate. This is suggested by our calculations in which the reaction coordinate in the neighborhood of the structure in Fig. 7 was probed without observing a significant energy change. It is important to note that in order to make quantitative predictions for the ratio of the 1,2-d_2-ethylene molecules that would retain their original configuration to those that do not retain their original configuration, a measure of the time required for the equilibration of *cis* and *trans* versions of the adsorbate is needed, as well as a measure of the lifetime of the structure shown in Fig. 7. Due to the low lifetime of these species on the surface it is very difficult to design an experiment that would allow for these measurements to be obtained. It is reasonable to expect that both of these characteristic times are highly dependent on the temperatures, pressures, adsorbates present on the surface, and electronic properties of the surface. The variety of results shown in Table 1 are likely a consequence of the

different experimental conditions and contact times at which the experiments were performed in different laboratories.

5.2. Rate-determining step in the steady state catalytic process

A common practice in the investigation of any catalytic process is an attempt to identify a rate-determining step. It is important to note that the understanding of elementary steps along a reaction coordinate is often not enough to pinpoint a rate-determining step. The reason is that, during any catalytic process, multiple effects such as the coverage of surface species, the interactions between them, or the need for accessible neighboring sites in some reaction pathways, may play roles not easily captured by microkinetic analysis. However, there have been a few attempts aimed at extracting rate-determining steps from calculated or experimentally determined reaction coordinates [43–45]. The analysis that is presented here is based on DeDonder relations [43,46]. The elementary steps in the reaction coordinate of Fig. 6 and respective rates can be written

$$\text{step 1}\quad O_2 + 2^* \leftrightarrow 2O^*$$
$$r_1 = k_1 P(O_2)[^*]^2(1 - z_1), \tag{3}$$
$$\text{step 2}\quad 2(C_2H_4 + {}^* \leftrightarrow C_2H_4{}^*)$$
$$r_2 = k_2 P(C_2H_4)[^*](1 - z_2), \tag{4}$$
$$\text{step 3}\quad 2(O^* + C_2H_4{}^* \leftrightarrow C_2H_4O^* + {}^*)$$
$$r_3 = k_3[O^*][C_2H_4{}^*](1 - z_3), \tag{5}$$
$$\text{step 4}\quad 2(C_2H_4O^* \leftrightarrow C_2H_4O + {}^*)$$
$$r_4 = k_4[C_2H_4O^*](1 - z_4), \tag{6}$$

where $P(O_2)$ and $P(C_2H_4)$ are gas phase partial pressures of O_2 and C_2H_4, respectively, and $[*]$, $[C_2H_4{}^*]$, $[O^*]$, and $[C_2H_4O^*]$ are the respective fractions of empty, ethylene-covered, oxygen-covered, and oxametallacycle-covered surface sites. We define z_1, z_2, z_3, and z_4 as the reversibility of steps 1, 2, 3, and 4, respectively:

$$z_1 = [O^*]^2 \big/ K_{1\text{eq}} P(O_2)[^*]^2, \tag{7}$$
$$z_2 = [C_2H_4{}^*] \big/ K_{2\text{eq}} P(C_2H_4)[^*], \tag{8}$$
$$z_3 = [C_2H_4O^*] \big/ K_{3\text{eq}} P(C_2H_4)[O^*], \tag{9}$$
$$z_4 = P(C_2H_4O)[^*] \big/ K_{4\text{eq}}[C_2H_4O^*], \tag{10}$$
$$z_{\text{total}} = P(C_2H_4O)^2 \big/ K_{\text{eq}} P(C_2H_4)^2 P(O_2). \tag{11}$$

Combining (7)–(11), the following relationship relating reversibilities can be obtained:

$$z_{\text{total}} = z_1 {z_2}^2 {z_3}^2 {z_4}^2.$$

The quantities z_i are bounded by 0 and 1 as long as the elementary steps proceed in the forward direction. Values of z_i equal or close to 1 suggest that the particular elementary step i is in equilibrium, while values of z_i less than 1 suggest a rate-determining step. $K_{i\text{eq}}$ and K_{eq} are the respective equilibrium constants for each elementary step and for the overall reaction.

The overall site balance is

$$1 = [^*] + [O^*] + [C_2H_4{}^*] + [C_2H_4O^*], \tag{12}$$

which results in

$$[^*] = 1/\big(1 + \big(K_{\text{eq1}} P(O_2) z_1\big)^{1/2} + K_{\text{eq2}} P(C_2H_4) z_2 + K_{\text{eq3}}\big(K_{\text{eq1}} P(O_2) z_1\big)^{1/2} K_{\text{eq2}} P(C_2H_4) z_2 z_3\big). \tag{13}$$

The rates of elementary steps can now be expressed as a function of gas phase partial pressures and the fraction of the surface empty sites:

$$r_1 = k_1 P(O_2)[^*]^2(1 - z_1), \tag{14}$$
$$r_2 = k_2 P(C_2H_4)[^*](1 - z_2), \tag{15}$$
$$r_3 = k_3\big(K_{\text{eq1}} P(O_2)\big)^{1/2} K_{\text{eq2}} P(C_2H_4)[^*]^2 z_1^{1/2} z_2(1 - z_3), \tag{16}$$
$$r_4 = k_4 K_{\text{eq3}} {K_{\text{eq1}}}^{1/2} K_{\text{eq2}} P(O_2)^{1/2} P(C_2H_4) \times z_1^{1/2} z_2 z_3(1 - z_{\text{total}}/z_1 z_2 z_3). \tag{17}$$

The unknown values z_1, z_2, z_3, and r can be determined by solving Eqs. (13)–(17) by requiring steady-state conditions, $r = r_1 = r_2/2 = r_3/2 = r_4/2$.

Table 3 shows the DFT-calculated values for pre-exponential factors and activation energies for each elementary step. The pre-exponential factors are calculated as derived from transition state theory. The in-depth derivations for pre-exponential factors for unimolecular and multimolecular reactions can be found in Moore and Pearson [47]. The partition functions and entropies of each species are calculated at 1 atm and 298 K using the ADF cluster approach. The pre-exponential factors for each elementary step are estimated from the partition functions by assuming minimal loss of degrees of freedom of reactant, products, transition states, and surface intermediates. To establish a certain level of confidence in the calculated values, we have used the data for step 1, the dissociative adsorption of oxygen, to estimate a sticking probability for this process at the low coverage

Table 3
Kinetic parameters for ethylene epoxidation on Ag

Elementary step	A_{for} [a]	$E_{a_{\text{for}}}$ [b]	A_{rev} [a]	$E_{a_{\text{rev}}}$ [b]
$O_2 + 2^* \rightarrow 2O^*$	5×10^6	17.3[c]	4×10^{13}	32.3[c]
$C_2H_4 + {}^* \rightarrow C_2H_4{}^*$[d]	10^6	0	10^{13}	8
$O^* + C_2H_4{}^* \rightarrow C_2H_4O^* + {}^*$	2×10^{11}	14.9	10^{13}	24
$C_2H_4O^* \rightarrow C_2H_4O + {}^*$	4×10^{13}	16	8×10^7	11

[a] Pre-exponential factors for forward and reverse reactions. Units are $\text{atm}^{-1}\,\text{s}^{-1}$ for adsorption and s^{-1} for desorption and surface reaction.

[b] Activation energies E_a for forward and reverse reaction; units are kcal/mol.

[c] From [25].

[d] The parameters for this step account for the weakly (~ 8 kcal/mol) adsorbed state of ethylene [32–34].

limit. This was done by equating the rate of dissociative adsorption of oxygen, as calculated by transition state theory in the low-coverage regime, with the rate of adsorption, as calculated from collision theory. The activation energy for the dissociative adsorption of O_2 at low coverage is calculated by using the activation barrier at 0.25 monolayer (included in Table 3) to extrapolate the activation barrier for 0.1 monolayer by taking advantage of the product-like nature of the transition state for oxygen dissociation. For example, the activation barrier calculated at 0.25 monolayer is 17.3 kcal/mol. According to Li et al. [26], the atomic oxygen on Ag is 5 kcal/mol per O_2 molecule more stable at 0.11 monolayer than at 0.25 monolayer. This implies that the activation barrier for oxygen dissociation at 0.11 monolayer is ca. 5 kcal/mol lower than at 0.25 monolayer. We obtain a sticking coefficient of $\sim 5 \times 10^{-5}$, which is in good agreement with experimentally measured zero-coverage values ranging from 3×10^{-5} to 3×10^{-3} [28,29,48–50] for different crystal planes of silver.

After the set of Eqs. (13)–(17) are solved, it is concluded that there are two kinetically relevant steps. Dissociative adsorption of oxygen and addition of weakly adsorbed ethylene to the oxygen-covered sites on the Ag surface appear to be kinetically relevant steps in the steady state catalytic process. Estimated values for z_1 (reversibility of dissociative adsorption of oxygen) and z_3 (reversibility of the addition of weakly adsorbed ethylene to an oxygen-covered site) are two to three orders of magnitude smaller than z_2 (reversibility of ethylene adsorption) and z_4 (reversibility of the surface intermediate reaction to form ethylene oxide). The investigation was done for multiple sets of conditions. The temperature was varied between 490 and 560 K with the total pressure between 1 and 5 atm with compositions ranging from 30 to 70% of oxygen and 70 to 30% of ethylene.

In order to obtain a quantitative measure of the kinetic relevance of each step we have also performed a sensitivity analysis for each [45]. In this analysis the forward and backward rates of an elementary step i are increased by 5% while everything else in the system, including the equilibrium constant for each step, is kept constant. The effect of this change on the reaction rate is defined by the ratio of the percentage change of the total rate divided by the percentage by which the particular elementary step was changed, i.e., 5%. This ratio represents the sensitivity of the total rate to a perturbation of the rate of a particular elementary step i. A higher sensitivity implies a kinetically "more relevant" step. We estimate that the sensitivity of the reaction rate with respect to the dissociative adsorption of oxygen is 0.8, while it is 0.2 with respect to the addition of ethylene to oxygen-covered sites. While this suggests that O_2 dissociation is rate-determining, it is clear that the surface reaction of oxygen atoms with ethylene is also kinetically relevant. The sensitivities of the rate with respect to ethylene adsorption and the product desorption steps are ~ 0, implying that these steps are not kinetically relevant. The existence of equilibrium for the desorption step implies a possible multiple sampling of the adsorbate state shown in Fig. 7 which, as was suggested, might be a precursor for rotation about the C–C bond, therefore making *cis*/*trans* isomerization more facile. The temperature used in this study was 530 K, with partial pressures of oxygen and ethylene of 2 atm each. The sensitivity analysis is consistent with the conclusion suggested above, indicating that there are two kinetically relevant steps. It is important to note that either of these steps can be rate-determining depending on the chosen conditions; that is, the identity of the rate-determining step can change for different temperatures and partial pressures. We illustrate the dependence of sensitivity on temperature in Fig. 8. Sensitivity factors for steps 1 and 3 are plotted as a function of temperature at which steady-state process takes place. The variation of sensitivities with temperature in Fig. 8 is fairly small, which is consistent with the similar activation barriers for these two steps.

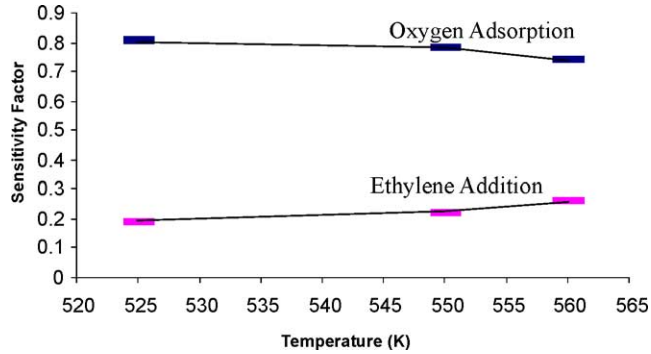

Fig. 8. Sensitivity of the reaction to oxygen dissociation and ethylene addition to an oxygen covered site as a function of temperature. The partial pressures of oxygen and ethylene are 1 atm each.

In order to compare quantitative calculated reaction rate, r, to the rates measured in a steady state catalytic process, r_m, information about the number of surface sites is required. However, since the measured reaction rate, r_m, will be equal to the reaction rate computed in our model multiplied by a constant (C), $r_m = Cr$, we can use the model to estimate the apparent activation energies for an Arrhenius expression of the overall rate without knowing the active site concentration. We calculate the rate from our model, r, as a function of temperature, keeping everything else in the system constant. For a power law rate expression with an Arrhenius form of the rate constant, r_m can be expressed as

$$r_m = Cr = k_{\text{overall}} P(O_2)^n P(C_2H_4)^m;$$
$$k_{\text{overall}} = A \exp(-E_a/RT), \tag{15}$$

where r_m is a rate measured for the steady state catalytic process, r is the rate calculated using our model, A is the pre-exponential factor, E_a is the apparent activation energy, $P(O_2)$ and $P(C_2H_4)$ are oxygen and ethylene partial pressures, and m and n are orders of reaction with respect to reactants, while C is a proportionality constant that accounts for the lack of knowledge about the number of available active sites.

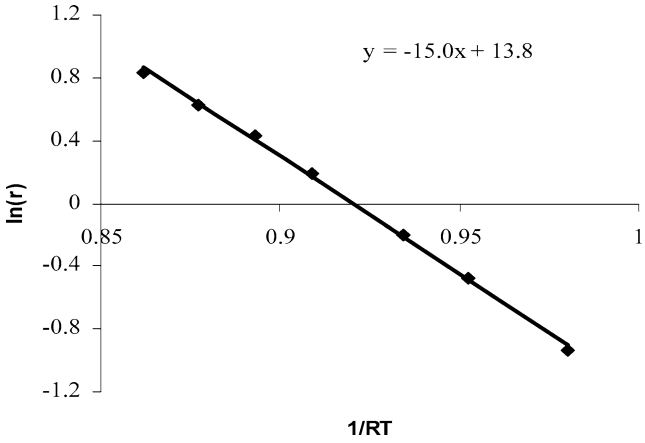

Fig. 9. Plot of natural logarithm of the reaction rate computed using the microkinetic model (see text), as a function of the inverse temperature, $1/RT$. The slope of the line represents the observable activation energy in kcal/mol if an Arrhenius expression for the rate constant is used in the kinetic analysis. The partial pressures of oxygen and ethylene are 1 atm each.

By taking the natural logarithm of Eq. (15) one obtains

$$\ln(r) = -E_a/RT + \ln(A) + n\ln\big(P(O_2)\big) + m\ln\big(P(C_2H_4)\big) - \ln(C). \quad (16)$$

Fig. 9 shows a plot of the natural logarithm of the rate of olefin consumption, as calculated by the kinetic model, as a function of the inverse temperature, $1/RT$. The slope of the line in Fig. 9 represents the apparent activation energy. We also note that the unknown variables, such as the number of available sites and order of the reaction with respect to either reactant, are captured in the intercept of the line shown in Fig. 9. We calculate the apparent activation energy to be 15 kcal/mol, which is in excellent agreement with activation barriers reported in various experimental studies, as shown by Table 4. The analysis described above suggests that in order to design an active ethylene epoxidation catalyst there has to exist an environment in which the dissociation of oxygen is facile, and the atomic oxygen formed on the surface is electrophilic enough to selectively attack the ethylene double bond. The interplay between these requirements, while making sure that selectivity towards ethylene oxide is kept at a certain level, is what governs the performance of a catalyst as measured by the yield of ethylene oxide. Any improved catalyst would have to satisfy these criteria.

Table 4
Apparent activation energies for the formation of EO

E_a (kcal/mol)	Reference
15	(this work)[a]
22	[11][b]
14	[59][b]
17	[60][b]
12	[51][b,c]

[a] Calculated for the proposed kinetic model.
[b] Observed in the steady state ethylene epoxidation process.
[c] Unpromoted silver catalyst.

Similarly to the estimation of the apparent activation barrier, we have also estimated the reaction order with respect to ethylene and oxygen. These orders are estimated with respect to the reactant consumption only through the pathway shown in Fig. 6; i.e., possible different parallel pathways, or pathways that might lead to different products, are disregarded. We estimate an order with respect to oxygen of 0.71 for partial pressures of oxygen varying from 1 to 5 atm with an ethylene partial pressure of 1 atm and a temperature of 560 K. This predicted order compares reasonably well with the value of 0.78 that was measured by Kestenbaum et al. [51] under similar experimental conditions in a steady-state catalytic process in which unpromoted silver catalyst was used in a microreactor setup. A similar calculation of the reaction order with respect to ethylene yielded an order of 0.65. The partial pressure of oxygen was kept at 1 atm, and the temperature at 560 K. The partial pressure of ethylene was varied between 0.1 and 1 atm. Kestenbaum et al. obtained an order of 0.53 for conditions identical to those applied in this microkinetic study. We compare the prediction of the microkinetic model to the results of Kestenbaum et al. mostly because the measurements obtained in their studies were obtained on unpromoted silver catalyst.

Since, as noted above, there exists a level of uncertainty in the calculation of activation barriers for dissociative adsorption of oxygen depending on which functional is used, we also implemented the above proposed microkinetic model to calculate the apparent activation energies and sensitivity factors as a function of the activation energy for oxygen dissociation. The temperature was 550 K, and partial pressures of ethylene and oxygen were set at 1 atm each. This analysis is shown in Fig. 10. It can be observed that the activation barrier for oxygen dissociation plays a crucial role in determining the respective kinetic relevance of the elementary steps. If the barrier for oxygen dissociation is less than 13 kcal/mol, ethylene addition to an oxygen-

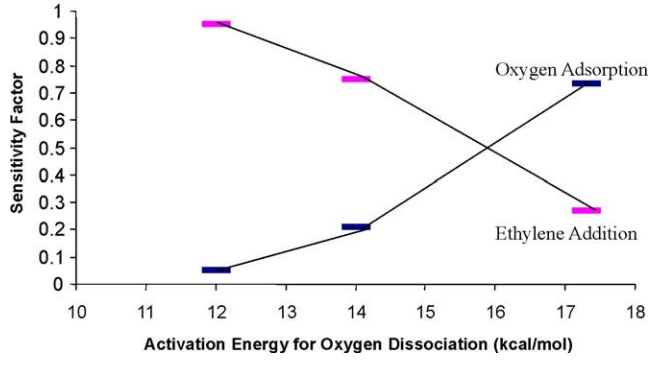

Fig. 10. Sensitivity factors as a function of the activation energy for oxygen dissociation. Energy units are kcal/mol. The partial pressures of oxygen and ethylene are 1 atm each; temperature is 560 K.

covered site is kinetically the most relevant step, while for activation barriers higher than 17 kcal/mol the dissociative adsorption of oxygen becomes the rate-determining step. This analysis is also important in view of the fact that the barrier for oxygen dissociation depends on oxygen surface coverage; higher coverages are associated with a higher activation barrier as discussed above. This suggests that for cases with total pressures above 2 atm in which the ethylene-to-oxygen ratio is high (> 4), i.e., the oxygen surface coverage is low, the surface reaction will be rate-determining due to the low activation barrier for oxygen dissociation. For the cases in which the ethylene-to-oxygen ratio is low (< 1) i.e., higher oxygen surface coverages, the dissociative adsorption of oxygen will become kinetically more important. Since most of the industrial processes are run (for safety reasons) in an ethylene-rich environment outside of the flammability region, it is expected that in these systems the surface reaction will be kinetically more relevant, as was suggested by Kung [52]. If the reaction is run in a reactor that allows high oxygen partial pressure and therefore higher oxygen coverage, for example a microreactor [51], the dissociative adsorption of oxygen is expected to be the more kinetically important step. The strong influence of the activation barriers on the kinetic relevance of elementary steps indicates that in order to obtain quantitative information about the kinetic behavior of a catalytic system, a high degree of computational accuracy in needed. This requirement stems from the exponential dependencies of rate laws on the activation barriers. It is also worth noting that the apparent activation energies for the overall reaction did not dramatically change for different activation barriers for oxygen dissociation within the limits of our investigation. This is in accord with the above-presented thesis of two kinetically relevant steps.

It is interesting to discuss the catalytic activity from the perspective of Sabatier's principle. Sabatier's principle states that the maximum rate of a catalytic reaction is found at an optimum catalyst-adsorbate interaction strength. Weak adsorbate–surface interaction leads to adsorption being rate-limiting, while strong interaction leads to desorption becoming the limiting process. At the optimum adsorbate–surface interaction, the rates of dissociative adsorption, surface reaction, and desorption tend to balance. Our analysis offers an explanation as to why silver is a good catalyst for ethylene epoxidation. The silver–adsorbate interaction, in particular the silver–oxygen interaction, is strong enough to facilitate the dissociation of oxygen and weak enough to allow oxygen–ethylene surface reaction and the facile ring closure of the oxametallacycle surface intermediate, resulting in the formation of gas-phase ethylene oxide.

Another intriguing issue of interest in any catalytic process is the selectivity of the process to a particular desirable product. In the case of ethylene epoxidation, silver is a unique metal with the ability to selectively facilitate this process. We provide a possible explanation for this using arguments that originate in the reaction coordinate shown in Fig. 6. First, it is reasonable to assume that the selectivity of ethylene epoxidation is governed by the conversion of the structure shown in Fig. 4 into gas ethylene oxide. The next step is to assume that the identities of the intermediates and transition states involved in the reaction coordinate would not significantly change on other metal surfaces, such as Group VIII transition metals. Due to the depletion of the d valence electron band and the higher energy of d electrons for Group VIII transition metals, it is expected that the surface intermediates, including the structure in Fig. 4, would adsorb more strongly on Group VIII metal surfaces than on Ag [53]. This would result in a more endothermic conversion of the surface structure into gas-phase ethylene oxide. According to the Brønsted–Polanyi relation this would result in a higher activation energy associated with this particular step on Group VIII metal surfaces compared to the activation energy on Ag. This would inevitably lead to a possibility of the other, unfavorable, reaction pathways being accessible, therefore leading to lower selectivity to ethylene oxide. This supports the previous suggestions of Mavrikakis et al. [18] in which the unique ability of silver to epoxidize ethylene was attributed to uniquely weak bonding of the surface oxametallacycle intermediate shown in Fig. 4 to silver metal. These conclusions were derived from calculations in which the stability of the surface oxametallacycle was evaluated on different metal clusters.

Another possible explanation for the unique ability of silver to facilitate ethylene epoxidation is that ethylene oxide formed from the oxametallacycle structure shown in Fig. 4 rapidly departs from the surface. It is reasonable to expect that more active metals, such as group VIII metals, would induce greater readsorption of product ethylene oxide. Adsorbed ethylene oxide is expected to bond more strongly to group VIII metals than to silver, which eventually might lead to its destruction. This argument is consistent with the observations made on Pd(110) [54,55], K/Ni(111) [56], and Pt(111) [57] in which the adsorption of EO resulted in its destruction and the formation of either CO and hydrogen on Pt(111) and Pd(110) or acetaldehyde on K/Ni(111).

In discussing ethylene epoxidation, it is important to note that promoters such as cesium and chlorine play an important role in making this catalyst selective and therefore industrially viable. Even though promoters play an important role in the process it can be said that they are not likely, particularly in small concentrations, to strongly influence the geometries of the structures existing along the reaction coordinate, i.e., to change the reaction mechanism. The promoters are more likely to change the thermodynamic stabilities of the surface intermediates and transition states with respect to each other and therefore to influence the activities of catalytic surfaces and the selectivity to specific products. It is speculated that in ethylene epoxidation, the presence of chlorine produces a net reduction of electron density on adsorbed oxygen, making it more electrophilic and therefore more efficient in the reaction with weakly adsorbed ethylene molecules. This argument can be explained from the view-

point of bond order conservation. Since O and Cl are both electrophilic when adsorbed on the surface, they compete for the surface electron density. The higher reactivity of oxygen is induced by its need to compensate for the electron density lost to Cl. This would suggest that the activation energy for the reaction of ethylene and adsorbed oxygen would be lowered compared to the case in which no chlorine is present, assuming that oxygen dissociation is not inhibited by the presence of chlorine. The same arguments that apply for Cl would also apply for surface or subsurface oxygen present on the catalyst during the steady-state catalytic process. We note that oxygen and chlorine have similar electron affinities.

It has also been observed that Cs increases the selectivity to ethylene oxide. The mechanism by which Cs acts is not clear. Our analysis suggests that in order to improve the selectivity to ethylene oxide, the promoter has to influence the energetics of step 3 in the reaction coordinate proposed here. We are in the process of studying the mechanism by which this might occur and will address this in more detail in future communications.

6. Conclusions

DFT calculations have been used to investigate the reaction coordinate for ethylene epoxidation on silver, and to develop a microkinetic model for this process from first principles. It was concluded that ethylene reacts with adsorbed oxygen to form a surface intermediate, previously identified as a surface oxametallacycle [5]. This intermediate reacts to form gas-phase ethylene oxide. A possible reason for the unique ability of silver to selectively catalyze ethylene epoxidation stems from the fact that silver provides a binding environment that is strong enough to dissociate oxygen but weak enough to allow for facile surface reaction and desorption of ethylene oxide. The proposed kinetic model suggests that in the steady state catalytic process the dissociation of oxygen and the reaction of weakly adsorbed ethylene with an oxygen-covered site are the kinetically relevant steps. The data obtained from the model are used to extract the kinetic parameters for a rate law. These parameters agree very well with the results of steady-state macroscopic measurements.

Acknowledgment

We gratefully acknowledge the support of the US Department of Energy, Division of Chemical Sciences (Grant FG02-84ER13290).

References

[1] R.A. van Santen, H.P.C. Kuipers, Adv. Catal. 35 (1987) 265.
[2] R.B. Grant, R.M. Lambert, J. Catal. 92 (1985) 364.
[3] J.K. Norskov, Nature 414 (2001) 405.
[4] J.R. Hahn, W. Ho, Phys. Rev. Lett. 87 (2001) 166102.
[5] S. Linic, M.A. Barteau, J. Am. Chem. Soc. 124 (2002) 310.
[6] E.L. Force, A.T. Bell, J. Catal. 38 (1975) 440.
[7] J. Deng, J. Yang, S. Zhang, X. Yuan, J. Catal. 138 (1992) 395.
[8] C.T. Campbell, B.E. Koel, J. Catal. 92 (1985) 272.
[9] H. Nakatsuji, K. Takahashi, Z.M. Hu, Chem. Phys. Lett. 277 (1997) 551.
[10] N.W. Cant, W.K. Hall, J. Catal. 52 (1978) 81.
[11] A.L. Larrabee, R.L. Kuczkowski, J. Catal. 52 (1978) 72–80.
[12] W.F. Richey, J. Phys. Chem. 213 (1972) 76.
[13] E.J. Baerends, ADF, Version 1999.02.
[14] C.F. Guerra, J.G. Snijders, G. te Velde, E.J. Baerends, Theor. Chem. Acc. 99 (1998) 391.
[15] S.H. Vosko, L. Wilk, M. Nusair, Can. J. Phys. 58 (1980) 1200.
[16] A.D. Becke, Phys. Rev. A 38 (1988) 3098.
[17] J.P. Perdew, Phys. Rev. B 33 (1986) 8822.
[18] M. Mavrikakis, D.J. Doren, M.A. Barteau, J. Phys. Chem. B 102 (1998) 394.
[19] R.A. van Santen, Catal. Today 50 (1999) 511.
[20] J.W. Medlin, M.A. Barteau, J. Phys. Chem. B 105 (2001) 10054.
[21] B. Hammer, L.B. Hansen, J.K. Norskov, Phys. Rev. B 59 (1999) 7413.
[22] M.A. Barteau, R.J. Madix, Surf. Sci. 97 (1980) 101.
[23] S. Reiff, J.H. Block, Surf. Sci. 345 (1995) 281.
[24] P.A. Gravil, D.M. Bird, Phys. Rev. Lett. 77 (1996) 3933.
[25] J.K. Norskov, T. Bligaard, A. Logadottir, S. Bahn, L.B. Hansen, M. Bollinger, H. Bengaard, B. Hammer, Z. Sljivancanin, M. Mavrikakis, Y. Xu, S. Dahl, C.J.H. Jacobsen, J. Catal. 209 (2002) 275.
[26] W.X. Li, C. Stampfl, M. Scheffler, Phys. Rev. B 65 (2002) 075407.
[27] G. Rovida, J. Phys. Chem. 80 (1976) 150.
[28] M. Bowker, M.A. Barteau, R.J. Madix, Surf. Sci. 92 (1980) 528.
[29] H.A. Engelhardt, D. Menzel, Surf. Sci. 57 (1976) 591.
[30] W. Kollen, A.W. Czanderna, J. Colloid Interface Sci. 38 (1972) 152.
[31] M.A. Barteau, R.J. Madix, in: D.A. King, D.P. Woodruff (Eds.), The Chemical Physics of Solid Surfaces and Heterogeneous Catalysis, Vol. 4, Elsevier, Amsterdam, 1982, p. 96.
[32] C. Backx, C.P.M. deGroot, P. Biloen, Appl. Surf. Sci. 6 (1980) 256.
[33] X.L. Zhou, J. Phys. Chem. 96 (1992) 7703.
[34] D. Stacchiola, G. Wu, M. Kaltchev, W.T. Tysoe, Surf. Sci. 486 (2001) 9.
[35] G. Capriani, D. Loffreda, A. Corso, S. Gironcoli, S. Baroni, Surf. Sci. 501 (2002) 182.
[36] S. Linic, J.W. Medlin, M.A. Barteau, Langmuir 18 (2002) 5197.
[37] G.S. Jones, M. Mavrikakis, M.A. Barteau, J.M. Vohs, J. Am. Chem. Soc. 120 (1998) 3196.
[38] E.M. Shustorovich, Surf. Sci. Rep. 6 (1986) 1.
[39] B. Hammer, J.K. Norskov, in: R.M. Lambert, G. Pacchioni (Eds.), Chemisorption and Activity on Supported Clusters and Thin Films, Kluwer Academic, Dordrecht, 1997, p. 285.
[40] R. Hoffmann, Solids and Surfaces: A Chemist's View of Bonding on Extended Surfaces, VCH, Weinheim, 1988.
[41] C. Minot, M. van Hove, G.A. Somorjai, Surf. Sci. 127 (1982) 441.
[42] C. Zheng, Y. Apeloig, R. Hoffmann, J. Am. Chem. Soc. 1988 (1988) 749.
[43] J.A. Dumesic, J. Catal. 185 (1999) 496.
[44] J.A. Dumesic, J. Catal. 204 (2001) 525.
[45] C.T. Campbell, J. Catal. 204 (2001) 520.
[46] T. DeDonder, L'Affinité, Gauthier–Villars, Paris, 1927.
[47] J.W. Moore, R.G. Pearson, Kinetics and Mechanism, Wiley, New York, 1981.
[48] H. Albers, W.J.J. van der Wal, G.A. Bootsma, Surf. Sci. 68 (1977) 47.
[49] C.T. Campbell, Surf. Sci. 143 (1984) 517.
[50] H. Albers, W.J.J. van der Wal, O.L.J. Gijzeman, G.A. Bootsma, Surf. Sci. 77 (1978) 1.
[51] H. Kestenbaum, A.L. de Oliveira, W. Schmidt, F. Schuth, W. Ehrfeld, K. Gebauer, H. Lowe, T. Richter, D. Lebiedz, I. Untiedt, H. Zuchner, Ind. Eng. Chem. Res. 41 (2002) 710.

[52] H.H. Kung, Chem. Eng. Comm. 118 (1992) 17.
[53] M. Mavrikakis, M.A. Barteau, J. Mol. Catal. A 131 (1998) 135.
[54] R. Shekhar, M.A. Barteau, Surf. Sci. 348 (1996) 55.
[55] R. Shekhar, M.A. Barteau, R.V. Plank, J.M. Vohs, Surf. Sci. 384 (1997) L815.
[56] B. Nieber, C. Benndorf, Surf. Sci. 269/270 (1992) 341.
[57] C.T. Campbell, M.T. Paffett, Surf. Sci. 177 (1986) 417.
[58] C.T. Campbell, Surf. Sci. 173 (1986) L641.
[59] M. Akimoto, K. Ichikawa, E. Echigoya, J. Catal. 76 (1982) 333.
[60] H. Kanoh, T. Nishimura, A. Ayame, J. Catal. 57 (1979) 372.